

## CHAPTER 4

### **Electrochemical Investigation of Archaeal DNA Repair Proteins Containing [4Fe4S] Clusters**

## INTRODUCTION

Life on earth may be categorized by the division of organisms into three separate domains: eucarya, bacteria, and archaea (1). Some archaeal organisms are noted for their ability to exist and thrive in extreme environments and for their relatively evolutionarily close relationship to eukaryotes (2). Thus, the study of archaea, and of specific systems derived from archaea, can provide important clues about life under highly demanding conditions and in complex eukaryotic organisms that are otherwise difficult to study.

Given the unique properties of archaea, it is interesting to consider the question of how they protect their genomic material (3, 4). Some archaea can grow in the presence of radiation and other exogenous DNA damaging agents as well as at extremely high temperatures (2), which can greatly enhance the rate of spontaneous DNA damage reactions (5). Yet these organisms do not exhibit a higher mutation rate when compared with other microbes (6). While preliminary evidence indicates that archaea do harbor DNA repair systems, many of which bear sequence homology to eukaryotic or bacterial repair pathways, a full understanding of archaeal DNA repair has remained elusive (3, 4).

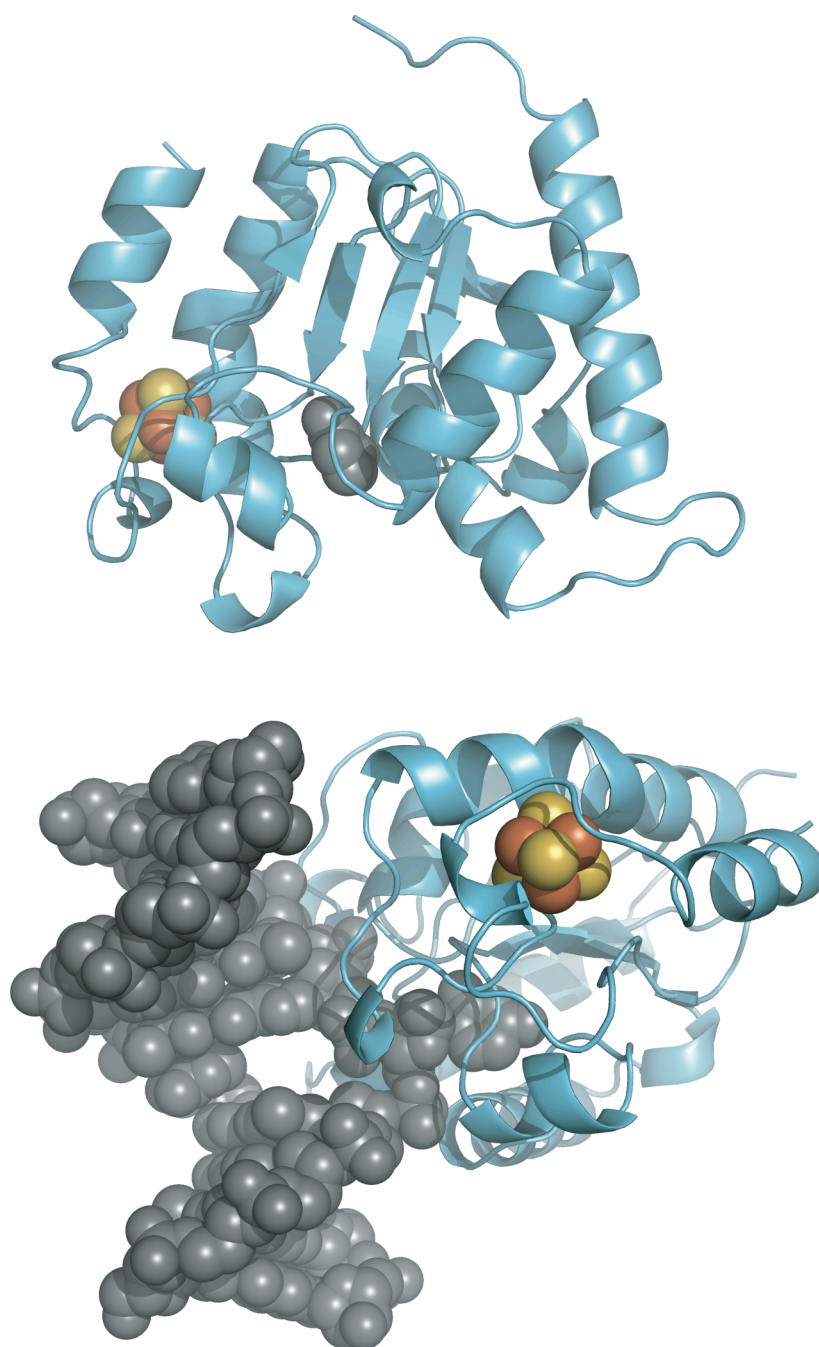
Base excision repair (BER) is the DNA repair pathway that is responsible for the excision of a variety of damaged DNA bases including uracil, oxidatively damaged bases (7,8-dihydro-deoxyguanosine and thymine glycol), methylated bases (3-methyl-adenine), and abasic sites (7, 8). Many archaeal organisms for which genomes have been sequenced, contain homologs of known BER enzymes from bacteria and eucarya (3, 4). Initially, one notable exception was the lack of any archaeal enzymes with homology to known enzymes that excise uracil in DNA in other organisms. Uracil in DNA arises via the misincorporation of uracil opposite adenine during replication or by the deamination

of cytosine to form G:U mispairs in DNA (9). Cytosine deamination is enhanced with increasing temperature (5), thus, it was surprising that archaea, especially hyperthermophilic archaea, did not possess a known uracil DNA glycosylase (UDG) homolog. Further examination of archaeal cell extracts revealed that archaea can, indeed, excise uracil from DNA (10) and it is now known that archaeal UDG enzymes constitute a new family of uracil excision enzymes termed family 4 UDGs. Several family 4 UDG genes have been isolated from archaea or expressed recombinantly in *Escherichia coli* (11-13). These are ~ 200 amino acid enzymes of extraordinary thermostability (enzyme activity can be maintained from 37–90°C) and the ability to remove uracil from G:U, A:U, and single stranded DNA environments.

Remarkably, many of these enzymes also contain [4Fe4S] clusters (14). Family 4 UDGs, as isolated, display a prominent absorption band between 370-400 nm and they lack any significant electron paramagnetic resonance (EPR) features at low temperature, an indication that the cluster exists in the [4Fe4S]<sup>2+</sup> state. Upon oxidation with ferricyanide, new EPR features arise at g values of 2.12 and 2.04, typical of a [4Fe4S]<sup>3+</sup> species. The cluster is ligated by a C-X<sub>2</sub>-C-X<sub>n</sub>-C-X<sub>14-17</sub>-C sequence where n = 70–100. This sequence does not resemble any other known iron-sulfur cluster ligation motifs.

Figure 1 shows the location of the iron-sulfur cluster in a *Thermus thermophilus* family 4 UDG homolog (15). *T. thermophilus* UDG adopts a  $\alpha/\beta/\alpha$  sandwich structure also found in the human UDG homolog. In Figure 1, the *T. thermophilus* UDG structure is aligned with that of human UDG bound to DNA (16). These alignments reveal that the [4Fe4S] cluster lies ~ 14 Å from the DNA backbone and ~ 10 Å from the active site uracil

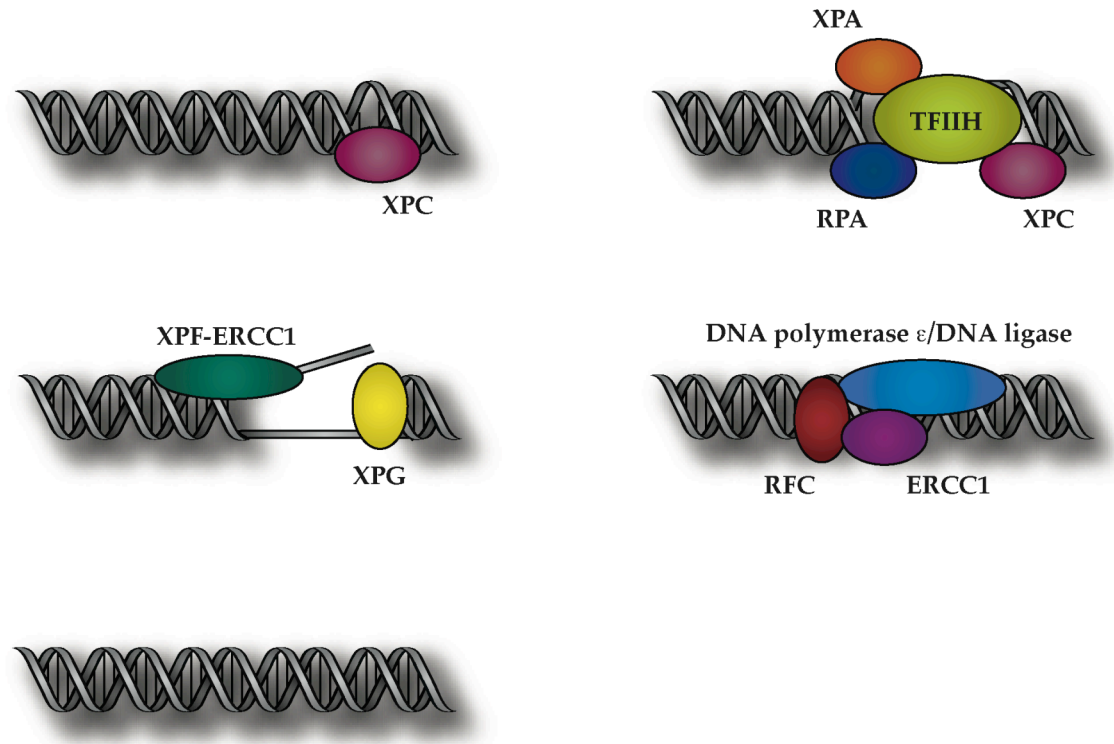
**Figure 4.1** A crystal structure of *Thermus thermophilus* uracil DNA glycosylase (UDG). *T. thermophilus* UDG adopts a  $\alpha/\beta/\alpha$  fold highly similar to that found in the human UDG homolog. A bound uracil nucleotide is shown in grey and the [4Fe4S] cluster is shown in yellow and orange. A structural alignment with the DNA-bound structure of the human UDG homolog is shown below. Note that the [4Fe4S] cluster in *T. thermophilus* UDG is located  $\sim 14$  Å from the DNA backbone in this model. Figure generated using 1UI0 and 1SSP PDB coordinates.



pocket. The role of the [4Fe4S] cluster remains unclear and the metal center has not been characterized in the DNA-bound form of the enzyme.

Another interesting feature of archaea is that they seem to lack the full complement of genes homologous to those involved in mismatch and nucleotide excision repair (NER) pathways in bacteria and eukaryotes (3, 4). NER is essential in bacteria and eukaryotes for the repair of DNA damage induced by UV light (17, 18). Archaeal organisms do possess some NER homologs that appear to be very similar to those present in eukaryotic NER systems (3, 4). In eukaryotes, global genomic NER is initiated by the XPC protein (Figure 2) which can recognize a wide range of lesions in DNA including UV damage products (thymine dimer, 6-4 photoproduct), DNA-protein crosslinks, and a variety of bulky DNA base adducts (19). XPC then recruits transcription factor IIH (TFIIH), replication protein A (RPA), and XPF-ERCC1. TFIIH is a multisubunit protein that contains the XPB and XPD helicases. XPB and XPD unwind the DNA around the damaged site, after which single strand DNA (ssDNA) binding proteins (RPA) are recruited as well as nucleases (XPG and XPF-ERCC1). These enzymes remove a 24–32 nucleotide swath of ssDNA containing the lesion. The last step in the pathway is the synthesis of new DNA. Understanding the biochemistry involved in eukaryotic NER poses specific challenges. Since many NER proteins exist as multiprotein complexes, it is difficult to isolate them individually and reconstitute NER *in vitro*. As with many other DNA repair pathways, it is also not well understood how NER enzymes very quickly and efficiently locate and repair damage in complex intracellular environments. It is generally accepted that XPC is the protein that initially detects damage inside the cell, but XPD and XPB helicases are also important for lesion recognition. Thus the discovery of archaeal NER homologs similar to eukaryotic NER enzymes could provide a much needed model system to understand this complex DNA

**Figure 4.2** Global genomic nucleotide excision repair (NER) in eukaryotes. NER is initiated by the XPC protein which binds to a wide variety of bulky DNA lesions. XPC then recruits the multisubunit protein TFIIH, which is responsible for verification of the lesion followed by unwinding of the helix in the vicinity of the damaged site. ssDNA binding proteins RPA and XPA are then recruited, followed by nucleases. The final step is synthesis of new DNA.



repair pathway. This is of the utmost importance since mutations in NER enzymes are associated with severe genetic disorders in humans including xeroderma pigmentosum, trichothiodystrophy, and Cockayne syndrome (20).

XPD homologs have been discovered in archaea through sequence analysis (21, 22). Initial characterization of *Sulfolobus acidocaldarius* XPD revealed that this archaeal XPD homolog harbors an iron-sulfur cluster (21). The purified protein has an absorbance maximum at ~ 410 nm and sequence alignments indicate that four cysteine residues are conserved across a large group of XPD homologs and related helicases, including several enzymes found in humans. EPR spectroscopy experiments show that exposure of *S. acidocaldarius* XPD to ferricyanide results in formation of a  $[3\text{Fe-4S}]^{1+}$  cluster observed at 10K. These properties are quite similar to those observed with the iron-sulfur clusters present in MutY, EndoIII, and family 4 UDGs (23, 24). Thus, it is likely that archaeal XPD homologs also contain a  $[4\text{Fe-4S}]^{2+}$  cluster. As with archaeal UDG, the iron-sulfur cluster in XPD has not been evaluated in the DNA-bound form of the enzyme.

## MATERIALS AND METHODS

### *Materials*

All chemicals were purchased from Sigma-Aldrich and used as received unless stated otherwise. All buffers were prepared immediately prior to use and filtered using a 0.2  $\mu\text{m}$  sterile filter. All reagents for DNA synthesis were purchased from Glen Research.

### *Proteins*

*A. fulgidus* UDG (AfUDG) variants were generously donated by Prof. Sheila David. *S. acidocaldarius* XPD was generously donated by Prof. Malcolm White (St. Andrews University).

### *Preparation of DNA-modified Electrodes*

Oligonucleotides were synthesized using standard phosphoramidite chemistry (25). Single strand oligonucleotides were modified at the 5' end with a thiol moiety to facilitate covalent attachment to a gold electrode surface, as described earlier (26). Oligonucleotides were purified by HPLC, hybridized to their complements and self-assembled into a loosely-packed monolayer on a Au surface (24) in 50 mM NaCl, 5 mM sodium phosphate, pH 7.0. The electrode surface was then further passivated by incubation with mercaptohexanol (100 mM) in assembly buffer for 30 minutes. Electrodes were then rinsed with protein storage buffer (AfUDG; 25 mM Tris-HCl, 500 mM NaCl, 5% glycerol, pH 7.6; XPD; 20 mM sodium phosphate pH 7.6, 250 mM NaCl, 1 mM EDTA, 10% glycerol), and 50  $\mu$ L protein (various concentrations) in the appropriate storage buffer was added to the electrode surface and allowed to incubate for 10–15 minutes prior to measurement.

### *Electrochemical Measurements*

Low volume constraints necessitated the use of a specialized low-volume cell for protein electrochemistry experiments (24). The working electrode consisted of a Au(111) on mica chip and a Pt wire served as the auxiliary electrode. The reference electrode was a Ag/AgCl electrode modified with a tip containing 4% agarose in 3 M

NaCl. This reference electrode was calibrated with ferrocene carboxylate and compared both to an unmodified Ag/AgCl reference electrode and a saturated calomel electrode. All measurements were made using a BAS CV50W model electrochemical analyzer.

## RESULTS AND DISCUSSION

### *A. fulgidus* UDG Electrochemistry

*A. fulgidus* UDG was investigated electrochemically at DNA-modified electrode surfaces (Figure 4.3). These electrodes were prepared as described previously (24, 26) and were modified with the sequence SH-(CH<sub>2</sub>)<sub>2</sub>CONH(CH<sub>2</sub>)<sub>6</sub>NHCO-5'-AGTACAGTCATCGCG-3' plus the complementary strand. All proteins were analyzed on loosely packed surfaces backfilled with mercaptohexanol. *A. fulgidus* UDG displays a strong electrochemical signal at DNA-modified electrodes (Figure 4.4) that is not present at electrodes modified with mercaptohexanol (24). The midpoint potential measured for the DNA-bound protein is +95 mV versus NHE, typical of high potential iron proteins that can access the 2+/3+ redox couple of the [4Fe4S] cluster (Figure 4.4). We have also examined a suite of *A. fulgidus* UDG single site mutants at each of the cysteines that ligate the iron sulfur cluster in the protein. C14, C17, C85, and C101 were each mutated to histidine, serine, or alanine. These twelve proteins were also examined on DNA-modified electrodes. With the exception of C14S, all mutants display an electrochemical signal when evaluated on a DNA monolayer. Representative cyclic voltammograms are shown in Figure 4.5 and the data is summarized in Table 4.1. All electrochemical signals measured for *A. fulgidus* UDG mutants share the same general characteristics as wild-type UDG and other [4Fe4S] cluster DNA repair proteins. The signals are quasi-

**Figure 4.3** Strategy for electrochemical analysis of iron-sulfur cluster DNA repair proteins at DNA-modified electrodes. DNA-modified electrodes are generated by self-assembly of thiol terminated DNA duplexes on a gold (Au) electrode surface to form a DNA monolayer. Electrodes are passivated with mercaptohexanol. Protein solutions are allowed to bind to the monolayer and evaluated with cyclic voltammetry.

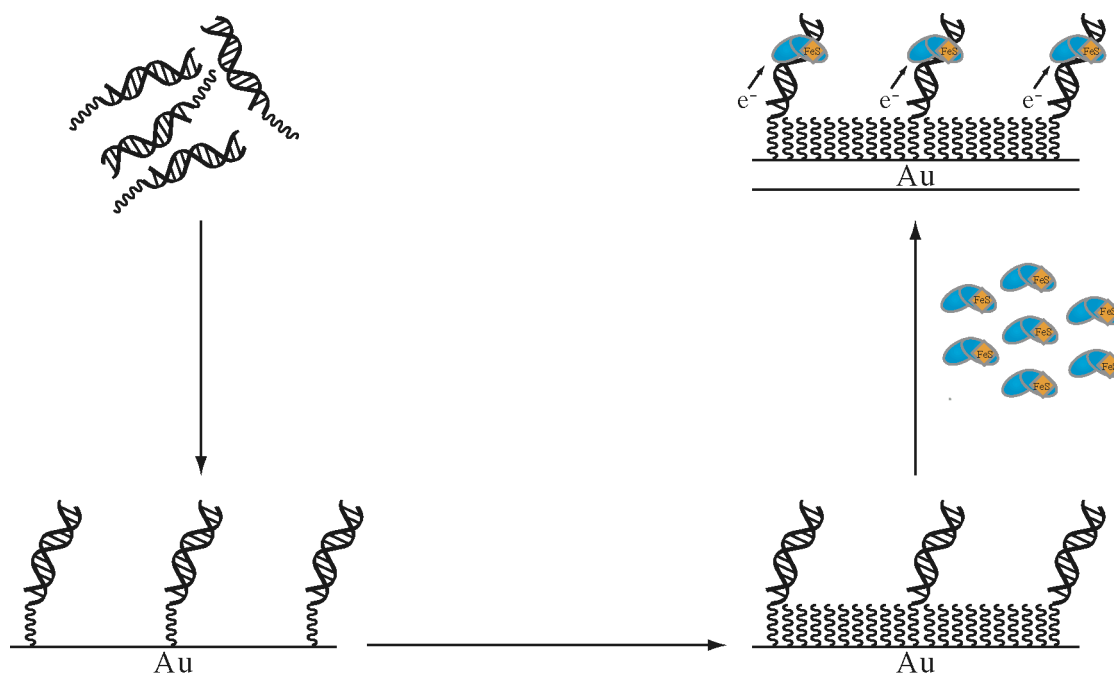


**Figure 4.4** Electrochemical investigation of *A. fulgidus* UDG at DNA-modified electrodes.

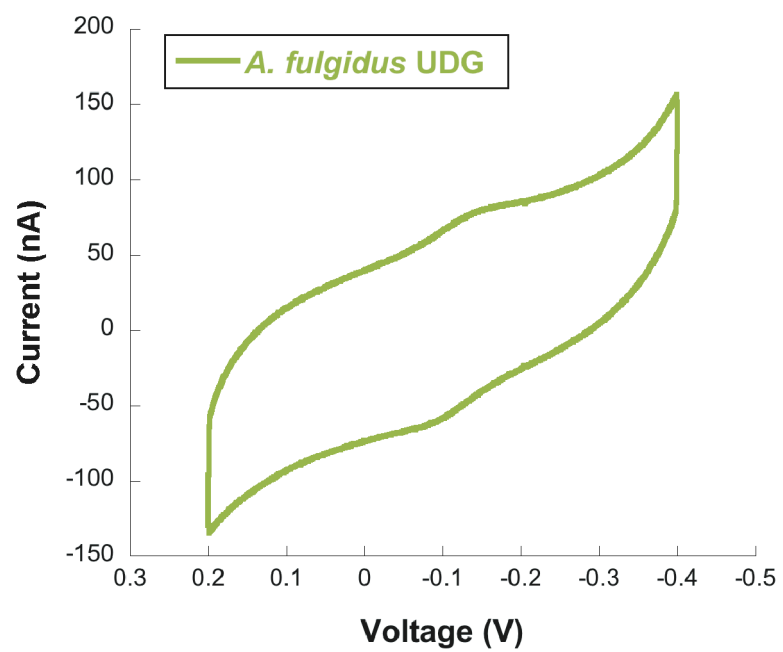


**Figure 4.5.** Cyclic voltammograms for the twelve *A. fulgidus* cysteine mutants evaluated electrochemically at DNA-modified electrodes.

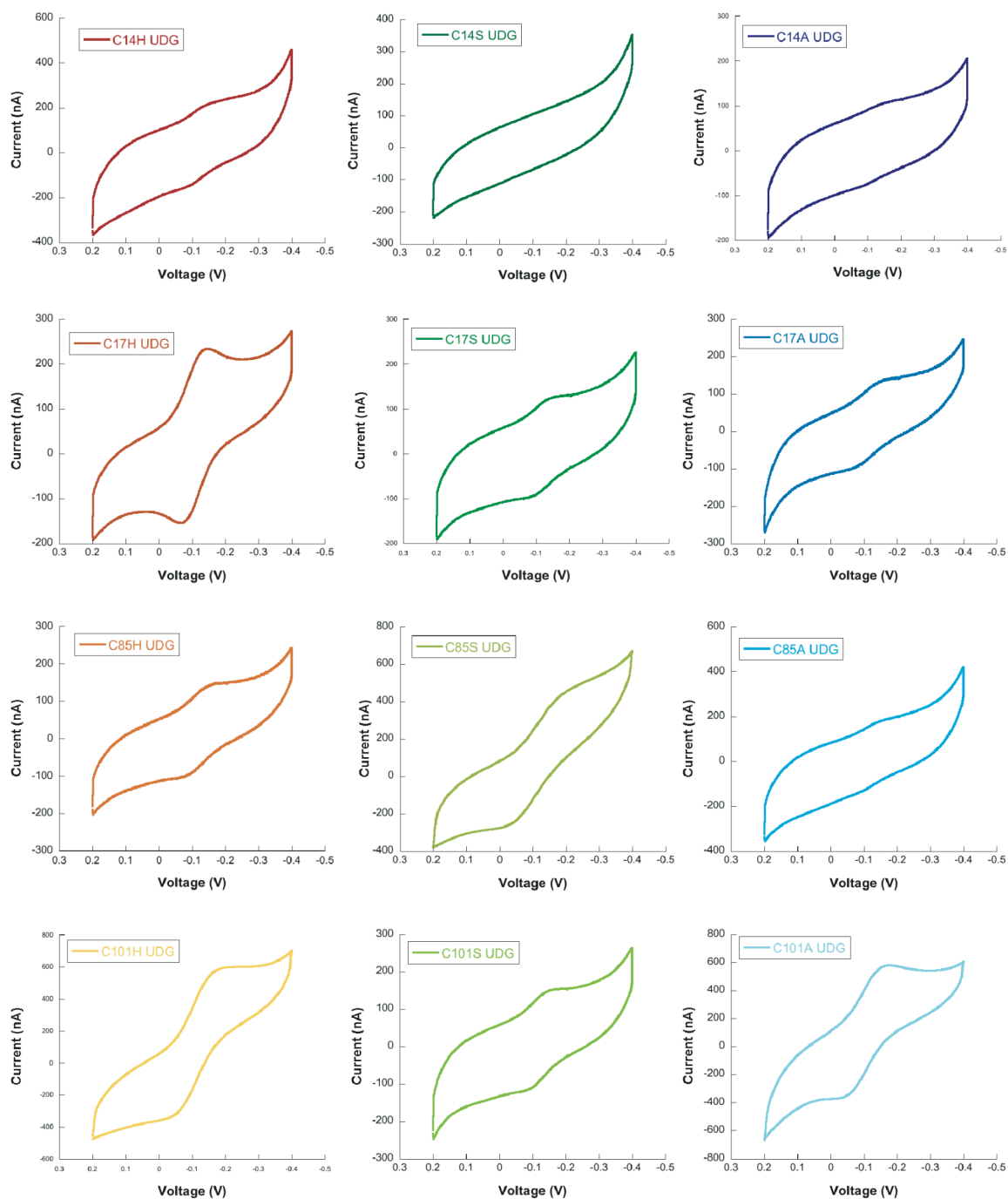


**Table 4.1.** Summary of electrochemical measurements for *A. fulgidus* UDG variants.

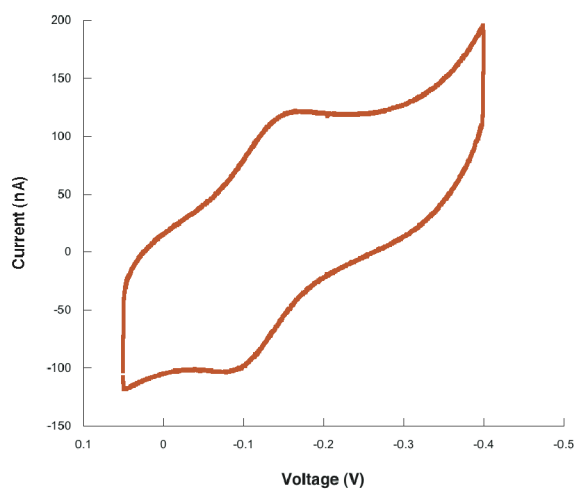
AfUDG mutant	$E_m$ (mV vs. NHE)	Intensity	Concentration	Distance to DNA
wt	+95 ± 3	+	170 μM	
C14H	+89 ± 5	-	100 μM	24 Å
C14S	--	N/A	498 μM	
C14A	+82 ± 4	-	384 μM	
C17H	+92 ± 3	+	100 μM	12 Å
C17S	+79 ± 3	+	200 μM	
C17A	+93 ± 5	-	150 μM	
C85H	+86 ± 5	-	400 μM	12 Å
C85S	+104 ± 9	-	200 μM	
C85A	+88 ± 7	-	140 μM	
C101H	+96 ± 6	+	200 μM	17 Å
C101S	+84 ± 3	+	200 μM	
C101A	+97 ± 4	+	200 μM	

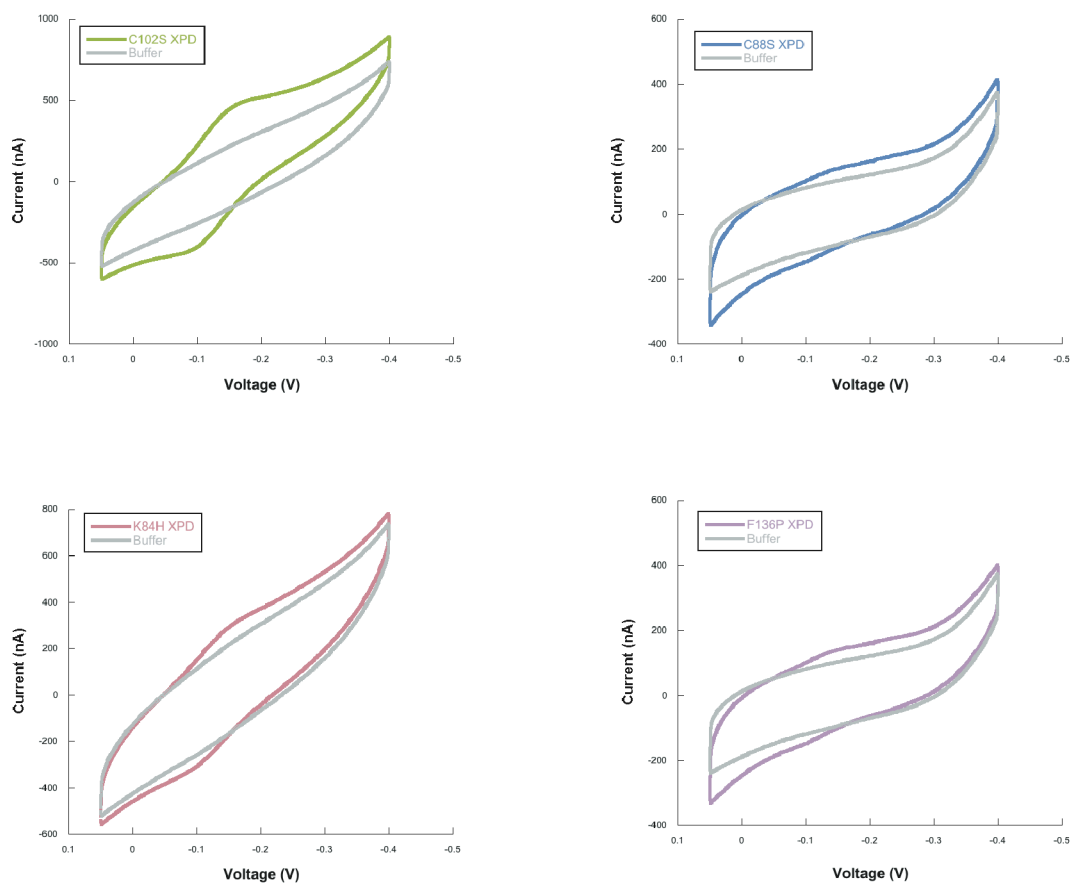
reversible, grow in on the order of 10–15 minutes, and have a linear relationship with respect to the square-root of the scan rate. Nearly all proteins display midpoint potentials similar to wild-type UDG with the notable exceptions of C17S, C101S, and C14A. Interestingly, the other serine ligated proteins either do not exhibit a signal (C14S) or have a slightly elevated midpoint potential (C85S). All of the alanine mutants examined, with the exception of C101A, display very weak signals, as might be expected since alanine cannot provide a ligation interaction to the iron-sulfur cluster. All of the histidine mutants have robust signals with midpoint potentials similar to that of wild-type UDG.

#### *S. acidocaldarius* XPD Electrochemistry

We have also examined *S. acidocaldarius* XPD on DNA-modified electrodes. XPD displays a quasi-reversible signal by cyclic voltammetry (Figure 4.6) when the protein is bound to DNA. The electrochemical signal associated with XPD also has many features in common with other [4Fe4S] cluster DNA repair proteins examined previously. The midpoint potential is +77 mV versus NHE, the XPD signal grows in over 10–15 minutes, and the peak current has a linear relationship with the square root of the scan rate. At an abasic site electrode, where DNA-mediated charge transport is hindered, XPD does not display a signal indicating that an intact  $\pi$ -stack is required for redox-activity of the enzyme (data not shown). Several mutant forms of XPD were also examined (Figure 4.7). C102S is an XPD mutant that still has an intact iron-sulfur cluster (21, 22) and it displays an electrochemical signal with similar properties to wt XPD. C88S, K84H, and F136P are mutants that do not appear to have an intact iron sulfur cluster (protein solutions are colorless) (21). These mutants exhibit electrochemical

**Figure 4.6.** Electrochemical investigation of XPD helicase at a DNA-modified electrode.



**Figure 4.7.** Electrochemical investigation of XPD variants.

signals on DNA-modified electrodes, though the integrated intensities of these signals are markedly smaller than those associated with wt or C102S XPD.

### *Discussion*

*A. fulgidus* UDG bears a [4Fe4S] cluster, much like the BER enzymes MutY and Endonuclease III (EndoIII) (14, 24). Though these enzymes all have a common cofactor, they are quite different in many other respects. *A. fulgidus* UDG has a very different overall fold when compared with MutY and EndoIII, as well as a different sequential spacing between the cysteines that ligate the iron sulfur cluster (15, 27, 28). MutY and EndoIII are members of the helix-hairpin-helix structural superfamily of DNA repair enzymes; they each have multiple domains and have a high degree of structural similarity to each other. The cysteines that ligate the iron-sulfur cluster in MutY and EndoIII are separated by a CX<sub>6</sub>CX<sub>2</sub>CX<sub>7</sub>C pattern that is unique to these enzymes. *A. fulgidus* UDG, however, is a single domain protein with a common  $\alpha/\beta/\alpha$  fold that is observed in a wide variety of proteins. This overall structure is similar to many other members of the UDG superfamily (15). The iron sulfur cluster in *A. fulgidus* UDG is ligated by a CX<sub>2</sub>CX<sub>67</sub>CX<sub>15</sub>C motif, a ligation pattern not found among known iron-sulfur enzymes. *A. fulgidus* UDG also has a very different substrate specificity when compared with MutY and EndoIII (11). MutY and EndoIII repair substrates associated with oxidative DNA damage (1), while *A. fulgidus* UDG removes uracil from DNA (11). Lastly, MutY and EndoIII are enzymes found throughout phylogeny (1), while *A. fulgidus* UDG and other family 4 UDGs that contain an iron-sulfur cluster are found largely in archaea (11-13).

In spite of these differences, the [4Fe4S] cluster in *A. fulgidus* UDG has many characteristics in common with the clusters found in MutY and EndoIII. In their isolated

forms, all of these proteins appear to bear a [4Fe4S] cluster in the 2+ oxidation state (24) demonstrated by the lack of any significant signal when these proteins are analyzed by EPR. These proteins do not exhibit strong EPR signals after reduction with sodium dithionite (14, 23). Following oxidation by ferricyanide, however, strong EPR features are observed. With *A. fulgidus* UDG, signals at  $g = 2.12$  and  $2.04$  indicate that both [4Fe4S]<sup>3+</sup> and [3Fe4S]<sup>1+</sup> species are formed upon oxidation. In MutY and EndoIII, ferricyanide treatment results in signals at  $g = 2.01$ – $2.03$  suggesting that only the [3Fe4S]<sup>1+</sup> species is present. This [3Fe4S] cluster is likely the result of oxidative degradation of the cluster or protein instability under the conditions required for EPR analysis (high protein concentration, extremely low temperature).

Electrochemical analysis of the [4Fe4S] cluster in DNA-bound *A. fulgidus* UDG also reveals similarities in the DNA-bound redox properties of *A. fulgidus* UDG and MutY/EndoIII (24). *A. fulgidus* UDG has a DNA-bound midpoint potential of +95 mV vs. NHE, comparable to those measured for MutY and EndoIII (+60–+90 mV versus NHE). *A. fulgidus* UDG redox activity is also sensitive to the integrity of the DNA  $\pi$ -stack, as are MutY and EndoIII. Thus, the pathway for electron transfer to the iron-sulfur cluster in these proteins is likely DNA-mediated.

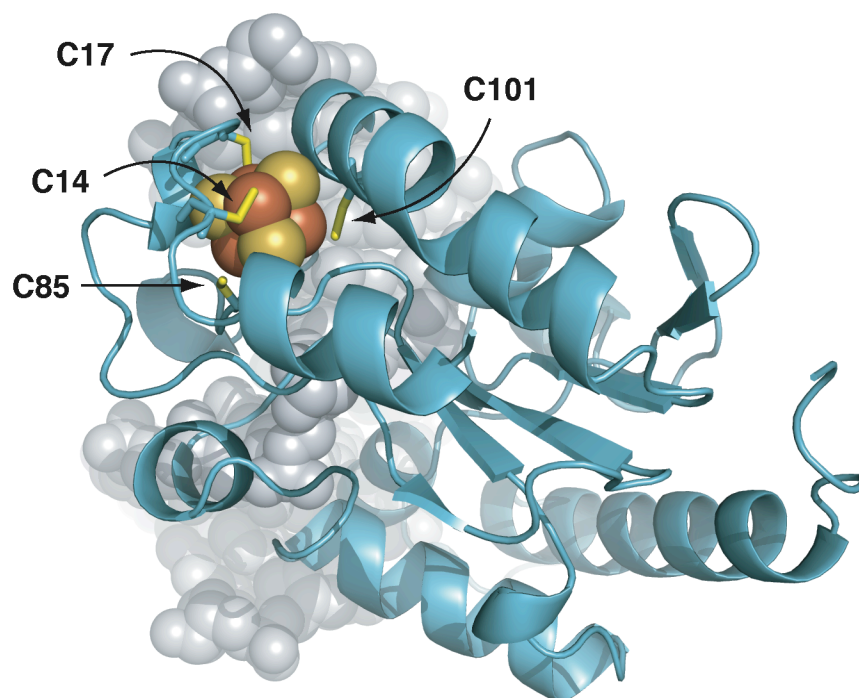
A complete set of *A. fulgidus* UDG mutants at residues that ligate the iron-sulfur cluster were also evaluated electrochemically at DNA-modified electrodes. Substitution of histidine at these sites leads to very little change in the redox properties when compared to wt *A. fulgidus* UDG. Though histidine is occasionally found as a natural ligand in protein bound [4Fe4S] clusters (29), histidine substitution for a thiolate ligand is often found to shift the midpoint potential of the iron sulfur cluster (30). Histidine substitution can also lead to cluster instability (31). Thus, the robust signals observed

here with little to no potential shift compared to wt UDG are a bit unusual and may indicate that iron-sulfur clusters in archaeal proteins have unique properties with respect to ligand substitution and redox activity.

Equally surprising are the effects of serine and alanine substitution for the cysteine ligands to the [4Fe4S] cluster in *A. fulgidus* UDG. Serine is not a natural ligand for [4Fe4S] clusters in proteins, but the hydroxyl group in the serine side chain does have some ability to bond with iron (30). Serine ligated [4Fe4S] clusters generated by site directed mutagenesis are generally unstable and may result in cluster degradation (32). In *A. fulgidus* UDG, three of the four serine mutants examined exhibit electrochemical signals when bound to DNA. Notably, two of these mutants (C17S and C101S) have midpoint potentials significantly lower (> 10 mV) than that of wt *A. fulgidus* UDG. The remaining mutant, C85S, does not exhibit a significant potential shift. Alanine substitution at all cysteines evaluated leads to small signals across the board with the exception of C101A. The observation of even very tiny signals is unexpected with alanine substitution, though, since the alanine side chain cannot serve as a ligand for iron. This result might indicate some small amount of cluster ligation by a solvent molecule or structural rearrangement by the protein to provide a new amino acid as a fourth ligand to the cluster. Indeed, the observation that all C101 mutants display strong signals regardless of the nature of amino acid substitution perhaps indicates that structural rearrangement is particularly favorable upon loss of the C101 ligand. Note that C101 is oriented towards the interior of the protein (Figure 4.8) and is likely the least solvent exposed of the four ligating cysteines (14).

It is also important to note that all of the measurements reported here were accomplished at room temperature while *A. fulgidus* is an organism that grows at extremely high temperatures (70–95 °C) (11). *A. fulgidus* UDG is an active enzyme over

**Figure 4.8.** View of the iron-sulfur cluster in a thermophilic family 4 UDG. The cysteine residues in *A. fulgidus* UDG are shown in yellow and labeled appropriately.



a wide range of temperatures, but it is certainly possible that observations made at room temperature may not reflect the properties of the protein in its native environment.

*S. acidocaldarius* XPD helicase is another iron-sulfur cluster enzyme found in archaea and involved in DNA repair (21). Sequence analysis indicates that iron-sulfur clusters are likely ubiquitous to many DNA helicases present in a broad range of organisms. While none of these helicases thought to contain iron-sulfur clusters have been structurally characterized, these enzymes likely have a very different structure and function from BER iron-sulfur cluster enzymes.

When evaluated at DNA-modified electrodes, *S. acidocaldarius* XPD displays a signal similar to those observed with MutY, EndoIII, and *A. fulgidus* UDG (24). The midpoint potential observed for *S. acidocaldarius* XPD (+77 mV versus NHE) at a DNA-modified electrode is within the range of that observed for DNA-bound [4Fe4S] cluster BER enzymes and typical of high potential [4Fe4S] cluster enzymes (32). As with the other [4Fe4S] enzymes, XPD requires an intact base-pair stack for efficient charge transport to the iron-sulfur cluster (data not shown).

The role of the iron-sulfur cluster in these helicases is unknown though it appears that the presence of an intact cluster is required for functional enzyme activity (21, 22). XPD helicase functions in the nucleotide excision repair pathway to unwind DNA in the vicinity of damaged sites (19). The general function of helicases and DNA translocases is to hydrolyze ATP and use the resulting energy to drive movement along the DNA helix or strand separation or both (33). Thus, the activity of these enzymes is characterized both by their ability to hydrolyze ATP or their ability to separate double stranded DNA substrates. In the XPD helicases containing iron-sulfur clusters, ATP hydrolysis is unaffected by loss of the iron-sulfur cluster through site-directed mutagenesis of the

residues ligating the cluster (21, 22). The cluster is, however, required for efficient strand separation of forked or bifurcated DNA substrates.

We have also examined several *S. acidocaldarius* XPD mutants on DNA-modified electrodes. C102S XPD maintains an intact iron-sulfur cluster and near wt activity for both ATP hydrolysis and strand separation enzyme functions (21, 22). When analyzed electrochemically at DNA-modified electrodes, C102S XPD has many features in common with wt XPD. The signal intensity and midpoint potentials measured for each protein are nearly identical. As with the *A. fulgidus* serine substituted mutants, the robust nature of C102S XPD is remarkable given that serine ligated [4Fe4S] clusters are prone to cluster degradation (32).

K84H, F136P, and C88S XPD mutants were also evaluated at DNA-modified electrodes. Though these XPD variants are deficient in strand separation activity and appear to have compromised iron-sulfur clusters (protein solutions are colorless) (21, 22), they do exhibit very small signals when monitored by cyclic voltammetry at DNA-modified electrodes. It is possible that only a very small proportion of these proteins contain intact iron-sulfur clusters and we are able to selectively detect these metal-bound proteins at the DNA surface.

For MutY and EndoIII, our laboratory has proposed that the redox-active [4Fe4S] cluster present in these proteins might allow these enzymes to take advantage of DNA-mediated charge transfer as a long-range damage detection method (24). Furthermore, this damage detection scheme could facilitate cooperative lesion detection among MutY and EndoIII, thus increasing the efficiency of damaged site location (34). It is interesting to consider that archaeal DNA repair enzymes bearing [4Fe4S] clusters might employ the metal center to perform a similar function. This principle is easily transferred to *A. fulgidus* UDG, since this BER enzyme plays a role quite similar to that of MutY and

EndoIII within the cell. Notably, *A. fulgidus* contains an EndoIII homologue (though it does not contain a MutY homologue) (35), allowing for the possibility of cooperative damage detection with EndoIII. It is interesting that the [4Fe4S] cluster is unique to family 4 UDGs, enzymes present in organisms that thrive at high temperatures where the formation of uracil in DNA is enhanced, leading to a greater requirement for UDG activity. Does the iron-sulfur cluster in these proteins help fulfill this need for greater DNA repair?

It is perhaps a bit less clear how XPD might use a redox-active iron-sulfur cluster in its function. XPD is part of the NER pathway and has a very different enzymatic function from that of the BER glycosylase enzymes discussed here. XPD and BER glycosylases do share a similar molecular recognition challenge within the cell. While XPD is not the initial damage recognition enzyme in NER (XPC plays that role) (19), it is recruited by XPC to damaged sites and this colocalization process is not well understood. Perhaps the iron-sulfur cluster in XPD could be used to harness DNA-mediated charge transport to locate XPC-bound lesions? Since XPD has a similar potential when compared to [4Fe4S] cluster BER enzymes, it may be possible that XPD could also participate in cooperative damage detection with these enzymes. Importantly, the iron sulfur cluster could be present in a wide range of XPD-related helicases found in a variety of organisms (21). Most of these helicases are not well characterized, but many of them are believed to function in DNA repair processes (33, 36). Thus, these enzymes may all be charged with the task of locating lesions, forked, looped, and bubbled DNA structures in a fast and efficient manner, a task which could be accomplished via DNA-mediated charge transport.

## SUMMARY

Several DNA repair enzymes from archaea have recently been discovered to contain iron-sulfur clusters. *A. fulgidus* UDG is a base-excision repair glycosylase, responsible for the excision of uracil in DNA, and the iron-sulfur cluster in this enzyme is unique to specific archaea. *S. acidocaldarius* XPD is a nucleotide excision repair helicase that unwinds DNA in the vicinity of bulky DNA lesions. The iron-sulfur cluster in this protein appears to be common to a large family of helicases present in many different organisms. *A. fulgidus* UDG and *S. acidocaldarius* XPD were both examined on DNA-modified electrodes to evaluate the DNA-bound redox properties of the proteins. *A. fulgidus* UDG displays an electrochemical signal at a DNA-modified electrode with a midpoint potential of +95 mV vs. NHE. A set of *A. fulgidus* UDG cysteine mutants were examined and nearly all of these variants have some DNA-bound redox activity indicating that this archaeal enzyme may be especially robust to ligand substitution at the iron-sulfur cluster. *S. acidocaldarius* XPD also exhibits DNA-bound redox activity with a midpoint potential of +77 mV versus NHE. The role of the [4Fe4S] cluster in these archaeal enzymes is unknown, but the redox properties of these proteins are quite similar to those of [4Fe4S] BER enzymes from *Escherichia coli*. For these *E. coli* enzymes, it has been proposed that the iron-sulfur cluster might allow BER enzymes to cooperatively search for damage via DNA charge transport. Perhaps the iron-sulfur cluster in archaeal UDG and DNA repair helicases has a similar function?

## REFERENCES

1. Neelson, K. H., and Conrad, P. G. (1999) *Phil. Trans. R. Soc. Lond. B* 354, 1923.
2. Pace, N. R. (1997) *Science* 276, 734.
3. Kelman, Z., and White, M. F. (2005) *Curr. Op. Microbiol.* 8, 669.
4. Grogan, D. W. (2004) *Curr. Issues Mol. Biol.* 6, 137.
5. Lindahl, T., and Nyberg, B. (1974) *Biochemistry* 13, 3405.
6. Jacobs, K. L., and Grogan, D. W. (1997) *J. Bacteriol.* 179, 3298.
7. David, S. S., and Williams, S. D. (1998) *Chem. Rev.* 98, 1221.
8. David, S. S., O'Shea, V. L., and Kundu, S. (2007) *Nature* 447, 941.
9. Lindahl, T. (1993) *Nature* 362, 709.
10. Koulis, A., Cowan, D. A., Pearl, L. H., and Saava, R. (1996) *FEMS Microbiol. Lett.* 143, 267.
11. Sandigursky, M., and Franklin, W. A. (1999) *Curr. Biol.* 9, 531.
12. Sandigursky, M., and Franklin, W. A. (2000) *J. Biol. Chem.* 275, 19146.
13. Sartori, A. A., Schar, P., Fitz-Gibbon, S., Miller, J. H., and Jiricny, J. (2001) *J. Biol. Chem.* 276, 29979.
14. Hinks, J. A., Evans, M. C. W., de Miguel, Y., Sartori, A. A., Jiricny, J., and Pearl, L. H. (2002) *J. Biol. Chem.* 277, 16936.
15. Hoseki, J., Okamoto, A., Masui, R., Shibata, T., Inoue, Y., Yokoyama, S., and Kuramitsu, S. (2003) *J. Mol. Biol.* 333, 515.
16. Slupphaug, G., Mol, C. D., Kavli, B., Arvai, A. S., Krokan, H. E., and Tainer, J. A. (1996) *Nature* 384, 87.
17. Setlow, R. B., and Carrier, W. L. (1964) *Proc. Natl. Acad. Sci. USA* 51, 226.
18. Setlow, R. B., Regan, J. D., German, J., and Carrier, W. L. (1969) *Proc. Natl. Acad. Sci. USA* 64, 1035.
19. Dip, R., Camenisch, U., and Naegeli H. (2004) *DNA Repair* 3, 1409.
20. Lehmann A. R. (2001) *Genes Dev.* 15, 15.

21. Rudolf, J., Makrantonis, V., Ingledew, W. J., Stark, M. J., and White, M. F. (2006) *Mol. Cell* 23, 801.
22. Pugh, R. A., Honda, M., Leesley, H., Thomas, A., Lin, Y., Nilges, M. J., Cann, I. K. O., and Spies, M. (2008) *J. Biol. Chem.* 283, 1732.
23. Cunningham, R.P., Asahara, H., Bank, J.F., Scholes, C.P., Salerno, J.C., Surereus, K., Munck, E., McCracken, J., Peisach, J., and Emptage, M.H. (1989) *Biochemistry* 28, 4450.
24. Boal, A.K., Yavin, E., Lukianova, O.A., O'Shea, V.L., David, S.S., and Barton, J.K. (2005) *Biochemistry* 44, 8397.
25. Beaucage, S. L., and Caruthers, M. H. (1981) *Tetrahedron Lett.* 22, 1859.
26. Kelley, S. O.; Boon, E. M.; Barton, J. K.; Jackson, N. M.; Hill, M. G. (1999) *Nucleic Acids Res.* 27, 4830.
27. Fromme, J. C., and Verdine, G. L. (2003) *EMBO J.* 22, 3461.
28. Fromme, J. C., Banerjee, A., Huang, S. J., and Verdine, G. L. (2004) *Nature* 427, 652.
29. Volbeda, A., Charon, M. C., Piras, C., Hatchikian, E. C., Frey, M., and Fontecilla-Camps, J. C. (2002) *Nature* 373, 580.
30. Venkateswara, R. P., and Holm, R. H. (2004) *Chem. Rev.* 104, 527.
31. Messick, T. E., Chmiel, N. H., Golinelli, M. P., Langer, M. R., Joshua-Tor, L., and David, S. S. (2002) *Biochemistry* 41, 3931.
32. Cowan, J. A., and Lui, S. M. (1998) *Adv. Inorg. Chem.* 45, 313.
33. Singleton, M. R., Dillingham, M. S., and Wigley, D. B. (2007) *Annu. Rev. Biochem.* 76, 23.
34. Boal, A. K., Genereux, J. C., Sontz, P. A., Gralnick, J. A., Newman, D. K., and Barton, J. K. (2008) (*submitted for publication*).
35. Klenk, H. P., *et al.* (1997) *Nature* 390, 364.
36. Voloshin, O. N., and Camerini-Otero, R. D. (2007) *J. Biol. Chem.* 282, 18437.